MECHANICAL AND THERMAL CHARACTERIZATION OF HTP FIBER REINFORCED LIGHTWEIGHT ENGINEERED CEMENTITIOUS COMPOSITES (HTP-LECC)

KAMILE TOSUN FELEKOĞLU[1], EREN GÖDEK[2] *

[1] *Dokuz Eylül University, Faculty of Engineering, Dep.of Civil Eng., İzmir, TURKEY*

[2]* *Hitit University, Vocational School of Technical Sciences, Dep. of Construction Technology, Çorum, TURKEY*

In this study, the matrix rheology, mechanical performances and thermal insulation properties of high tenacity polypropylene fiber (HTP) incorporated lightweight engineered cementitious composites were investigated. Matrices were prepared by using air entraining admixture 2, 4 and 8% of cement weight and HTP fibers added to matrices by 2% of total matrix volume. Before fiber addition, rheological properties of matrices were investigated by using a ball type rheometer. After fiber addition, the air entrainment percentages of composites were determined through theoretical calculations, aerometer test, and image processing methodology for comparison purpose. Specimens were cast into: 25x60x300 mm prismatic molds for flexural strength and thermal tests; dog-bone molds for tension tests; 50x50x50 mm cubes for compression tests. Crack numbers and crack widths of specimens were measured additionally to the mechanical test by using a portable hand microscope at unloaded state in order to investigate crack properties after flexural and tensile test. Thermal properties of composites were also investigated by thermal conductivity and thermal permeability measurements. The thermal conductivity values of composites were achieved by using prismatic specimens before flexural tests. Correlations between air-dry densities and thermal conductivities were calculated. Additionally, thermal permeability of composites were obtained by using a novel thermal camera integrated test setup, which simulates actual site conditions, and related with the thermal conductivity test results. In conclusion, composites were lightweightened by 19-35%. The accuracy of the aerometer test was confirmed by image processing technique. Yield stress and viscosity of matrices were decreased by increasing air entraining admixture dosage and 8% of air entraining admixture dosage was found much preferable in terms of consistency preservation. First crack (in both flexural and tensile tests) flexural, tensile and compressive strengths of composites were decreased by increasing air entrainment percentage. By taking air entrained composites into account, deflection and strain capacity of HTP-LECCs were increased by increased admixture dosage. Also, crack numbers were increased and crack widths were decreased by increasing admixture dosage within air entrained composites. Thermal permeability of composites were investigated by novel thermal camera test setup. Strong correlation (R=0.96) was found between thermal conductivity and thermal permeability tests.

Keywords: *Lightweight ECC, air entrainment, rheological, mechanical, thermal, HTP*.

Highlights

-The first lightweight ECC incorporating HTP fiber was produced and characterized
-Air entraining admixture dosage positively affected the rheology of cement matrix
-Deformation capacities of HTP-LECCs were enhanced by increasing admixture dosage
-Thermal permeability of HTP-LECCs were investigated by novel thermal camera test setup
-Strong correlation was found between thermal conductivity and permeability tests

1. Introduction

Engineered cementitious composites (ECCs) are polymeric fiber incorporating cement based composites and unlike traditional fiber reinforced concretes, exhibit strain hardening behavior owing to occurrence of multiple micro cracks with enhanced strength, deformation and toughness capacity. Last decades, various types of ECC have been developed for various structural applications. However, within these studies, increasing the mechanical performance of ECC is the common output [1-3].

Lightweight Engineered Cementitious Composite (LECC) is special type of ECC that incorporating air voids generated by air entraining agents, hollow glass spheres or hollow fly ash particles. LECC first introduced to the literature by Wang and Li [4]. The object of this study was to develop LECC with improved strain capacity and enhanced strength in both compression and tensile loading conditions. They used polyvinyl alcohol (PVA) fiber by 2% of total volume. For ensuring the lightweight criterion, they used air entraining agent, expanded perlite, glass bubbles and micro hollow bubbles. LECCs having densities between 0.93-1.78 were produced and their tensile strain capacity, tensile strength and compressive strength values ranged between 0.35%-4.24%, 1.91-4.56 MPa and 11.8-46.4 MPa, respectively. Thermal properties of LECCs were not investigated in this study. Huang et al. [5] further investigated thermal properties of green LECC (GLECC) in addition to the mechanical properties. In this study, tensile ductilities over 3.4% at relatively lower densities (1649–1820 kg/m^3) were obtained with reduced thermal conductivity values ranging between 0.278-0.370 W/m.K. Wu et al. [6] developed ultra- lightweight cement composites

* Autor corespondent/*Corresponding author*,
E-mail: erengodek@hitit.edu.tr

Table 1

Properties of binding materials

Chemical Analysis (%)		
	CEM I 42.5R	**Metakaolin**
SiO_2	18.57	54.93
Al_2O_3	4.95	41.00
Fe_2O_3	3.11	2.00
CaO	63.94	0.04
MgO	0.98	0.06
Na_2O	0.37	0.00
K_2O	0.75	0.21
SO_3	3.07	0.03
Loss on ignition (%)	3.57	0.08
Cl^- ion (%)	0.006	-
Insoluble residue	0.21	0.21
Serbest CaO	1.03	-
Physical Properties		
Unit weight	3.09	2.79
Blaine surface area (cm^2/g)	3370	23.96
Sieve retaining 90 µm	0.7	-
Sieve retaining 45 µm	19.3	7.8
Volume Stabilitiy (mm)	0.5	
Compressive Strengths (MPa)		
2 d	27.2	
7 d	39.9	
28 d	49.3	

Table 2

Properties of HTP fibers

Unit Weight	Length (mm)	Diameter (µm)	Modulus of Elasticity (GPa)	Tensile Strength (MPa)	Elongation at rupture (%)
0.91	10	12	6	850-900	21

Table 3

Proportions of ingredients (kg/m^3)

Composite Series	Cement	Water	Metakaolin	Limestone Powder	PCA	HTP fiber	AE
MK 0%AE (Control)	451	397	282	846	13.5	18	0
MK 2%AE							9
MK 4%AE							18
MK 8%AE							36

(ULCC) that incorporating polyethylene (PE) fiber by 0.5% of total volume. The compressive strengths of ULCC were between 33-69.4 MPa and thermal conductivities were ranged between 0.28-0.80 W/mK. Recently, Chen et al. [7] developed cenosphere incorporating PVA fiber reinforced high strength lightweight ECC (HSL-ECC) and observed 50 MPa of compressive strength, strain capacity of over 1% and thermal conductivity between 0.39-0.45 w/m.K.

The only literature that studied thermal property of ECC incorporating high tenacity polypropylene (HTP) fiber was studied by Zhang and Li [8]. They designed a fireproofing ECC material by using HTP fiber which was also suitable for spray applications. However, in this study lightweightness criterion was not considered.

In this study, HTP-LECCs were prepared by using air entraining chemical admixture by 2, 4 and 8% of cement weight and HTP fiber at the ratio of 2% by total volume. Rheological behaviors of matrices were investigated and mechanical performances of composites were tested. Crack analyses of composites were conducted and results were related with the mechanical parameters. Also, the thermal conductivity and thermal permeability of composites were investigated.

2. Materials and methods

CEM I 42.5R type cement and metakaolin were used as binding ingredients. Their chemical and physical (also mechanical for cement) properties were presented in Table 1. Limestone powder was used as micro aggregate having a unit weight of 2.69. Ether sulphate based air entraining chemical admixture (AE) according to ASTM C260 [9] standard was used. The unit weight of the AE was 1.01, and the alkali and sulphate ratios were 1.61% and 0.70% respectively. Polycarboxylate-based chemical admixture (PCA) was used in order to adjust the workability of fresh mixture. As fiber phase, new kind of polymeric micro fibers named as high tenacity polypropylene fibers (HTP) is used 2% by volume. Based on our initial studies with HTP fibers, dosages higher than 2% cause workability problems (fiber balling) and dosages less than 2% do not always guarantee the saturated multiple cracking of composites. A second reason for selecting the dosage of 2% is the economical advantage of polypropylene raw material which is easily available in the market. Physical and mechanical properties of HTP fibers were presented in Table 2. Mixture proportions of composites were given in Table 3. Preparation procedures of composites were presented in Figure 1.

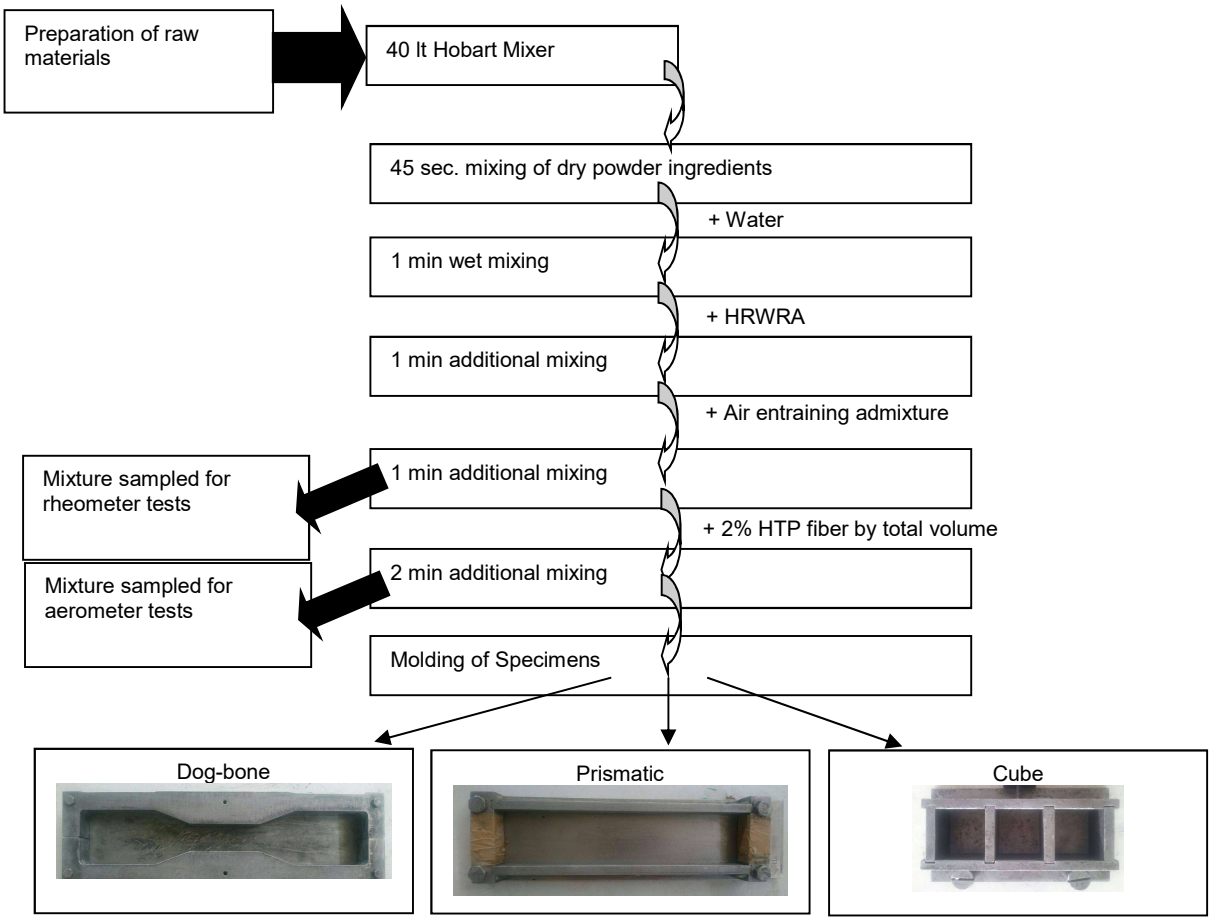

Fig. 1 - Preparation procedures of composites.

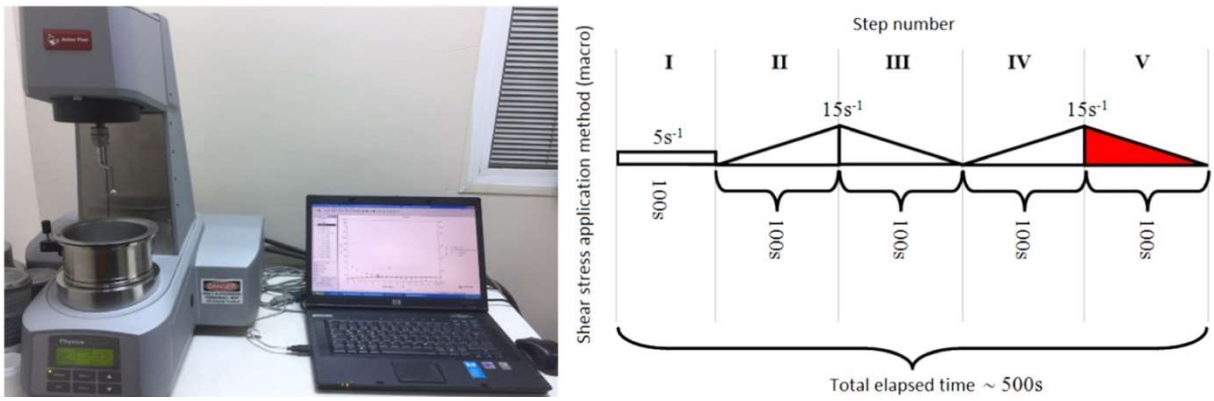

(a) (b)

Fig. 2 - a) Rheometer used in tests and b) Measurement macro.

2.1 Determination of Rheological Parameters

For investigating the effect of air entraining admixture dosage to the fresh state workability properties, 400 cm^3 of matrices were taken from the mixture during the mixing stage (Figure 1). In rheological tests, ball type rheometer (Anton Paar MCR51) with a diameter of 8 mm was used (Figure 2a). Shear stress – shear rate curves were achieved by using the data obtained from the final down of measurement macro owing 5 step shear rate (Figure 2b). Dragging resistance of 8 mm metal ball was measured during the rotation and used for torque calculations by Rheoplus software on the computer that integrated to rheometer. Torque values were converted to shear stress and rotation speeds were converted to shear rate by Schatzmann transformations [10]. For the details of measurement procedure readers referred to [11].

Rheological data were measured from the fresh mixtures at 5 and 45 min durations for investigating the consistency loss of matrices. By using the obtained data, flow curves of mixtures were drawn by using the data obtained from V. step of measurement macro which rheological behavior was believed to have become stable

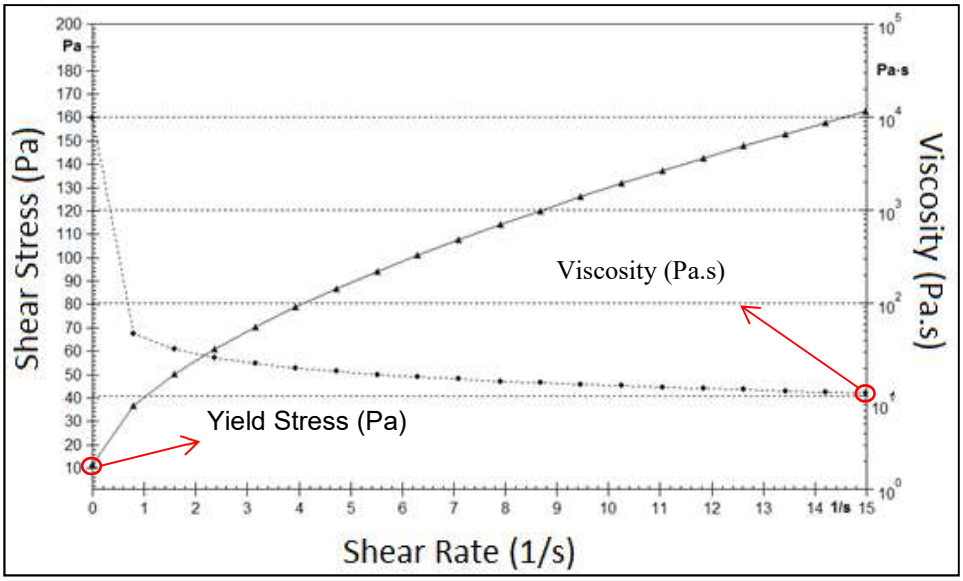

Fig. 3 - Method of yield stress and viscosity determinations from the flow curves.

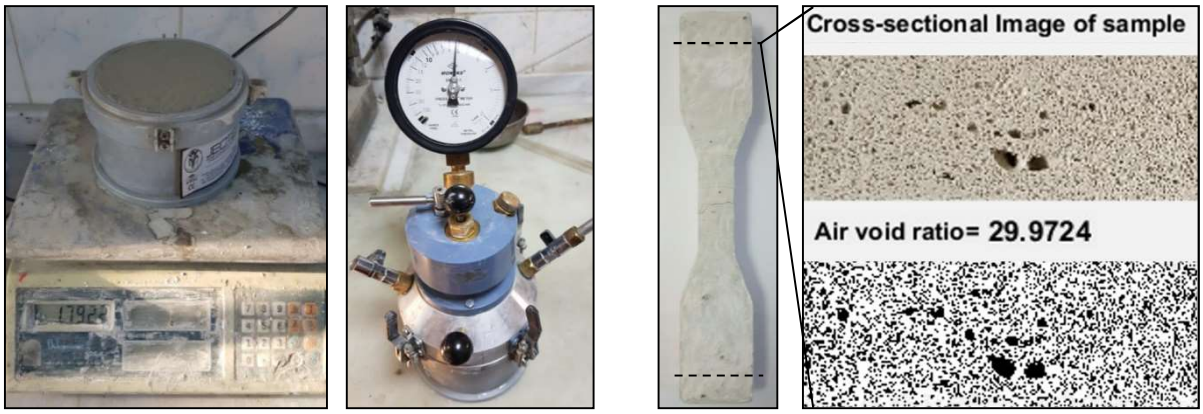

(a) (b) (c)

Fig. 4 - Determination of entrained air volume; a) Theoretical calculation, b) Aerometer test, c) Image processing methodology.

(a) (b)

Fig. 5 - a) Thermal conductivity test setup, b) Measurement method.

(Figure 3). The initial shear stress values of matrices were defined as yield stress (τ_0) and viscosities (η) were read at highest shear rate (15 s^{-1}) (Figure 3).

2.2. Determination of Entrained Air Volumes of Mixtures

In order to determine the entrained air volume of mixtures, three methodologies were used. After the addition of HTP fibers, 2 min additional mixing was applied to the fresh mixtures

1 dm^3 of sample from each mixture was taken and container belonging to aerometer was full filled. In first methodology, the fresh unit weight of mixture was calculated and subtracted from the theoretical weight of control mix. The percentage of the resultant to theoretical weight was determined as the air-entraining amount (Figure 4a). Then, aerometer tests were performed to mixtures for the air entraining values of mixtures were measured according to ASTM C 231 [12] as second methodology (Figure 4b). For the third

methodology, an image processing methodology based on Matlab algorithm was used. After the mechanical tests, undamaged end portions of the three tensile specimens were cut. 6 samples for each mixture were obtained. Images were captured from the cross-sections of cut samples than analyzed by Matlab. In matlab algorithm, images were converted to binary images. Pixels of light colored matrix were seen as white while the air voids were appeared as black. Numbers of white and black pixels were counted. The ratio of black pixels to the whole pixel number was determined as the air void ratio for each cut sample. The averages of these values within each mixture were calculated (6 edge for each mixture) and accepted as air-entraining amount of mixture (Figure 4c).

2.3 Determination of Air-Dry Densities

Remaining mixtures were cast into: 25x60x300 mm prismatic molds for flexural and thermal tests; dog-bone molds for tension tests; 50x50x50 mm cubes for compression tests (Figure 1). Specimens demolded after 1 day of casting and cured for 28 days in water. After curing, composites dried in air and their air dry unit densities were calculated by dividing the weight of specimen to volume of the specimen. Air dry densities of specimens were determined for each series by averaging the results.

2.4 Determination of Thermal Properties

After density measurements, thermal conductivity values of composites were determined on prismatic specimens. A quick thermal conductivity meter (Showa Denko K. K. – Shoterm QTM-D2) based on hot wire method confirming to ASTM C 1113 [13] was utilized for measuring thermal conductivity coefficients of composites (Figure 5a). Conductivity measurements were performed to each composite from the right, middle and left part of the composites (Figure 5b). Their averages were assumed as the thermal conductivity for each composite, individually.

Thermal permeability test setup includes an artificial heat source (owing digital temperature regulator and timer) and an infrared thermometer (Figure 6a). Technical specifications of the thermal camera were given in Table 4. The artificial heat source carefully designed in order to ensure homogeneous heat distribution to whole surface area of specimens (Table 5).

Measurement side of test setup consist of consists of 4 spaces adjusted in composite dimensions. First was used for measuring and verifying the surface temperature. Specimens were placed to the other three for thermal permeability measurements (Figure 6b). Heating temperature was adjusted, kept constant and checked by using infrared thermometer. Thermal permeability

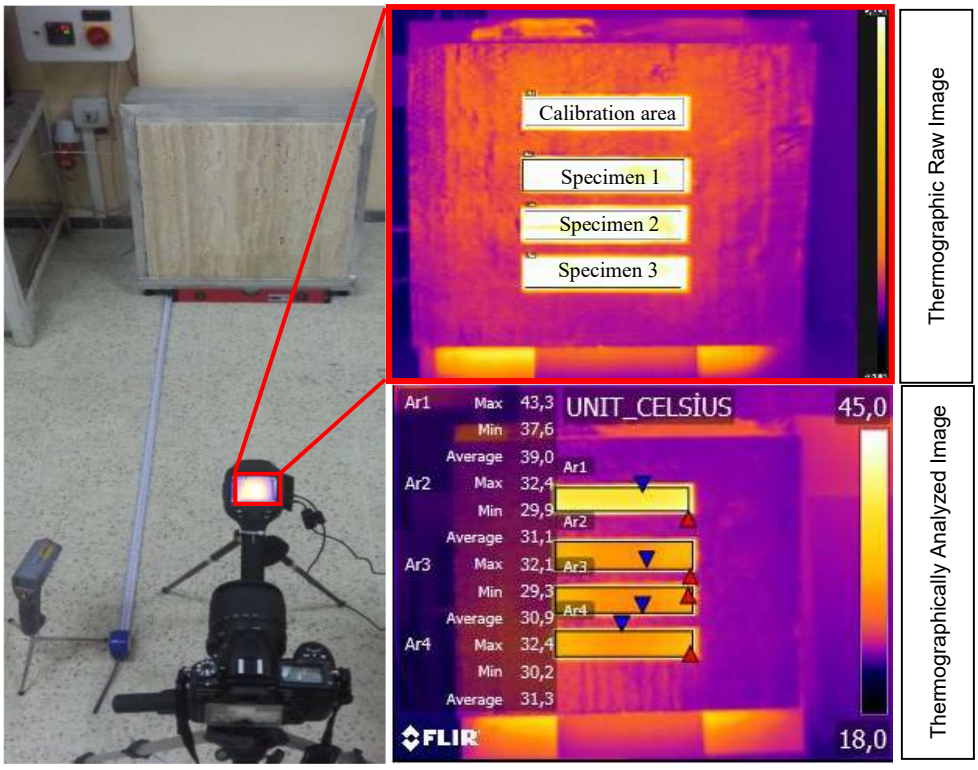

(a) (b)

Fig. 6 - a) Thermal permeability test setup, b) Thermographic analyses of composites.

Table 4

Properties of thermal camera

IR resolution of Thermal Camera	240 × 180 pixels
Sensitivity	< 0.05°C at +30°C
Field of view	25° × 19°
Focal length	18 mm
Type of detector	Uncooled microbolometer, focal plane array
Spectral range	7.5–13 µm
Accuracy	±2°C or ±2% of reading between temperatures 10-35°C

Table 5

Properties of heat source

Max. power	5000 W
Dimensions	70x70x30 cm
Adjusted current	5.5 A
Status	Fully insulated except the measuring surface

properties of composites have been investigated at 45°C degrees. Specimens initially conditioned at 23-24°C. Thermographic images were captured and recorded along 1 hour by 5 min intervals. Their thermographic analyses were examined with a software by taking whole area of the composite into consideration and the ultimate surface temperature (UST) after an hour exposure to heat was measured (Figure 6b). This value was assumed as an indicator of thermal permeability of composites where a low UST means improved thermal performance in terms of insulation.

2.5 Mechanical Tests

After the completion of thermal tests, mechanical tests were performed. 50 kN capacity of SHIMADZU tension device was used for tensile tests and tensile elongation rate of 0.5 mm/min was applied to the specimens. Linear variable displacement transducers (LVDTs) were placed to each corner of specimen. Load and elongation values were recorded by using the software on the test computer that connected to the tension device.

Middle part of the dog-bone specimen in 100 mm length was selected as measurement length for strain calculations (Figure 7a). Four-point flexural tests were conducted under controlled displacement (0.5 mm/min). A LVDT with a gage of 30 mm was placed to the mid-point and deflection values were recorded. The experimental setup is shown in (Figure 7b). Compressive strengths of specimens were achieved by compression device of 3000 kN. Loading rate during the compressive test was set to 907.5 N/sec.

The tensile stress-strain and flexural load-deflection graphs were plotted. By using these graphs, the first crack/tensile/flexural strengths, maximum unit strain (ductility), deflection capacity and compressive strength parameters of composites were determined (Figure 8). Loads corresponding to first crack initiation were obtained from the first non-linearity of graphs [14]. The first crack strength and flexural/tensile strength parameters were calculated by using the first crack and peak loads (equations were presented in Figure 8). The corresponding deflection/strain values to the peak load/peak stress were defined as deflection/strain capacity. Flexural peak toughness is accepted as the total area under the load-deflection curve until peak load [15].

Finally, the multiple cracking behaviors of composites and crack properties (width and number) were examined by using a digital portable hand microscope after the removal of applied load (unloaded state) at 250x magnification level. For this purpose, center line was drawn along the composites as being parallel to the long dimensions. Number of cracks intersecting with this line was accepted as crack number and the widths of cracks were measured. The averages of measured crack widths (except the major crack) was calculated and determined as the average crack width.

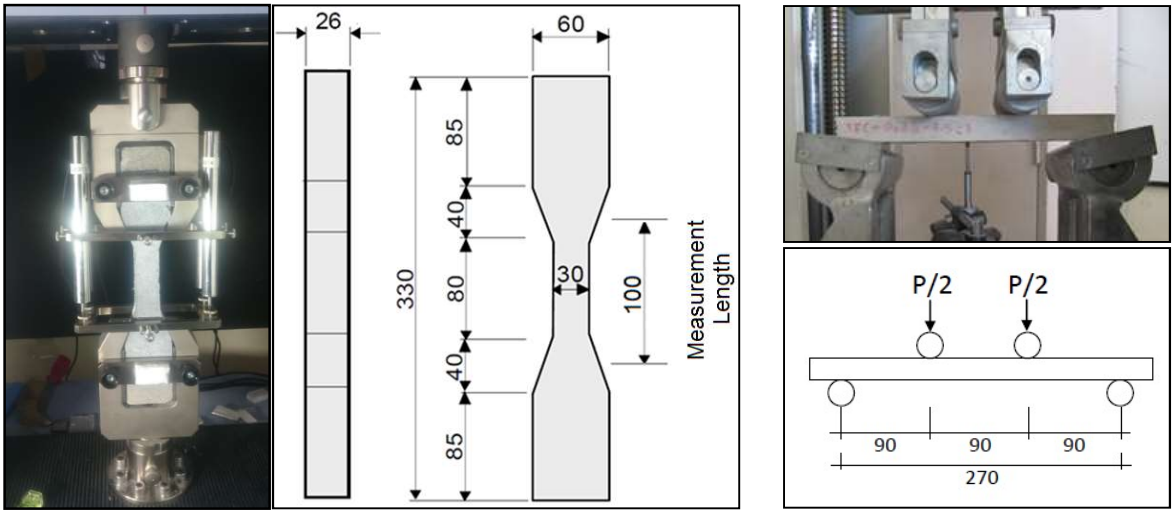

(a) (b)

Fig. 7 - Test setups a) Uniaxial tension, b) Four-point flexure.

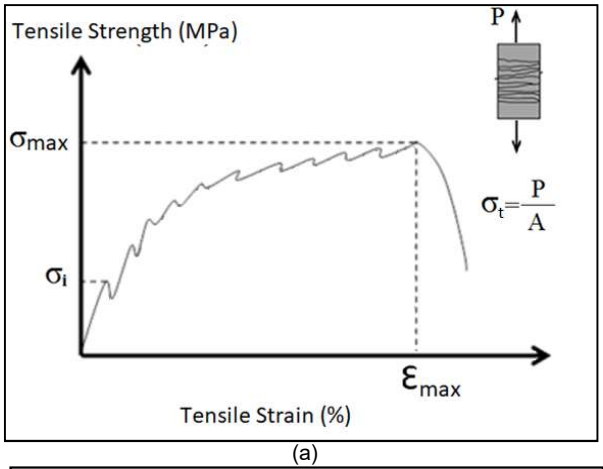

(a)

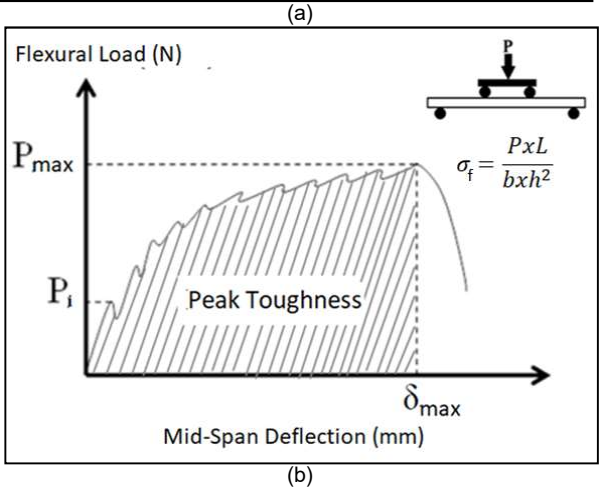

(b)

Fig. 8.- a) Tensile strength – Tensile strain graph, b) Flexural load – Mid-span deflection graph.

3. Results and discussion

3.1 Percentages of Air Entrainment

Changes in the air entrainment percentages of composites were presented in Figure 9 by taking both methodology and air entraining admixture dosage into account. The aerometer test results were defined as the reference methodology in this study since the methodology was standardized in ASTM C231 [12]. Other methodologies had been tried as a confirmatory method to ASTM C231 since there was no specific standard for determining the air entrainment percentages of fiber reinforced cement based composites.

In all methods, the air entrainment percentages of composites increased by air-entraining dosage as expected. Theoretical calculations were presented relatively higher values when compared with the image processing and aerometer test results. The air entraining amounts obtained from the image processing methodology was found compatible with the aerometer results. Note that, the aerometer test results will be taken into consideration for the discussions at the next parts of this study.

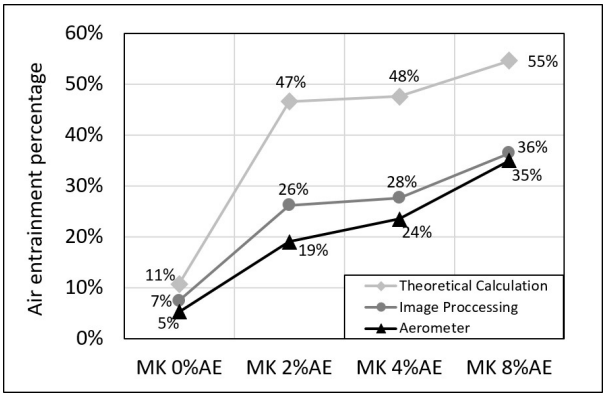

Fig. 9 - Amounts of entrained air in composites.

3.2 Rheology Test Results

Yield stresses (τ_0) and viscosities (η) of matrices were presented through dotted columns in Figure 10 at 0 and 45 min durations. Dots were used in accordance with the air entraining dosage for easily tracking the data.

At 0 min of rheology tests, τ_0 was slightly increased by 10 and 15% by using AE at dosages of 2 and 4%, respectively (Figure 10a). Further increasing the AE dosage to 8% remarkably decreased the τ_0 by 53%. Viscosity of matrix was also slightly increased by approximately 1% (Figure 10b). However, increasing the AE dosage up to 2% decreased the η of matrices. By using AE at the dosage of 4% decreased the η by 19%.

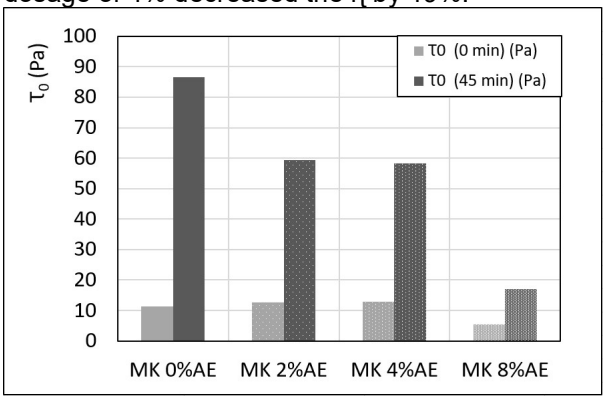

(a)

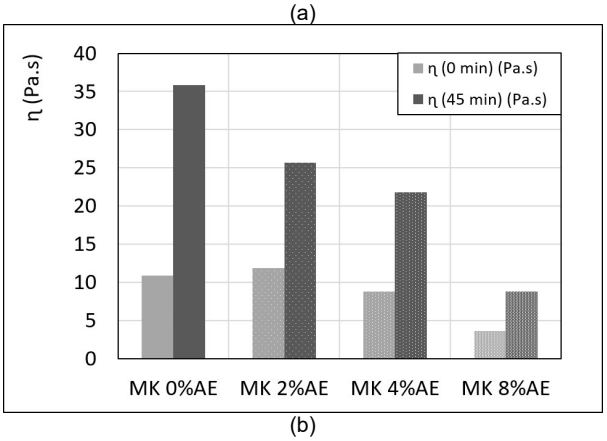

(b)

Fig. 10 - a) Yield stress values, b) Viscosity values.

Further increasing the AE dosage to 8% significantly decreased the η by 67% (Figure 10b).
45 min after first experiments, rheological behaviors of mixtures re-tested which is related to workability retention of mixtures. τ_0 values of matrices were increased as expected by 670, 371, 349 and 219% for 0, 2, 4 and 8% AE dosages, respectively. However, the increment ratio was decreased with increasing AE dosage (Figure 10a). Viscosities of matrices were gradually decreased by increasing the AE ratio. Viscosity increment ratios for 0, 2, 4 and 8% of AE ratio was also calculated as 230, 116, 148 and 143%, respectively (Figure 10b).

The use of AE, decreased both the τ_0 and η values when compared to control matrix. Relatively lower values in terms of both τ_0 and η was observed for the case of 8% air entraining admixture. Besides, slight increment was obtained over time elapsed (at 45 min experiments) when compared to other matrices. The use of 8% AE for achieving lower yield stress and viscosity is preferable. However, it must be noted that an optimum dosage value for AE should be determined in order to obtain not only the good workability but also the mechanical performance and thermal conductivity.

3.3 Mechanical Test Results

3.3.1 Flexural Test Results

The flexural load – deflection graphs, first cracking/flexural strengths and deflection capacities were presented in Figure 11a and Figure 11b, respectively. Observations for first crack/tensile strength can be made by using the left axis; strain observations can be made by using the right axis of Figure 11b.

First crack/flexural strengths decreased by increased AE dosage. With the addition of 2% AE, first crack/flexural strengths of composites significantly decreased by 47% (Figure 11a and 11b). Increasing the AE dosage up to 8% gradually decreased both first crack and flexural strengths. In terms of deflection capacities, non-regular results were obtained under flexural loading conditions and standard deviations were also increased. The use of AE by 2% decreased the deflection capacity. Use of AE by 4% increased the deflection capacity up to 8.67 mm (Figure 11b). Further increasing the AE dosage to 8%, deflection capacities of composites ranged between 4.57-9.91 mm (Figure 11b).

Since the flexural peak toughness value dependent to both load and deflection, flexural peak toughness – flexural strength - deflection capacity relations of composites were given in Figure 12. Both the flexural strengths and deflection capacities of control specimens were comparatively high and due to this reason control series gave the best results on flexural peak toughness. The flexural strengths of air entrained

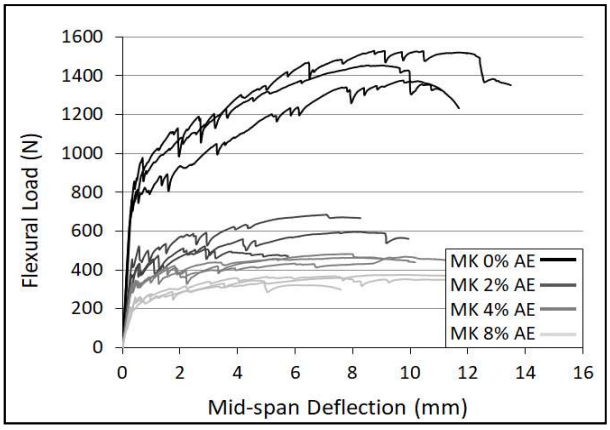

(a)

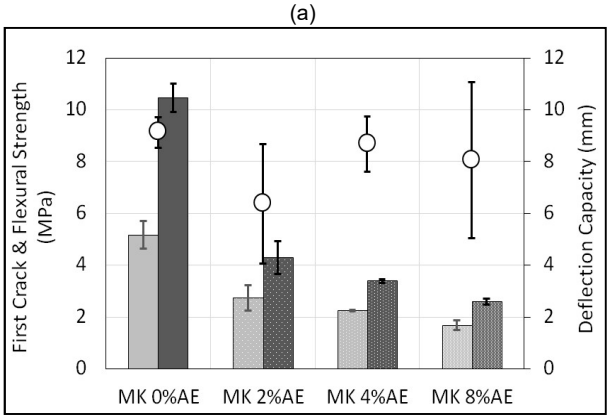

(b)

Fig.- 11. a) The flexural load – deflection graphs, b) First cracking/flexural strengths and deflection capacities.

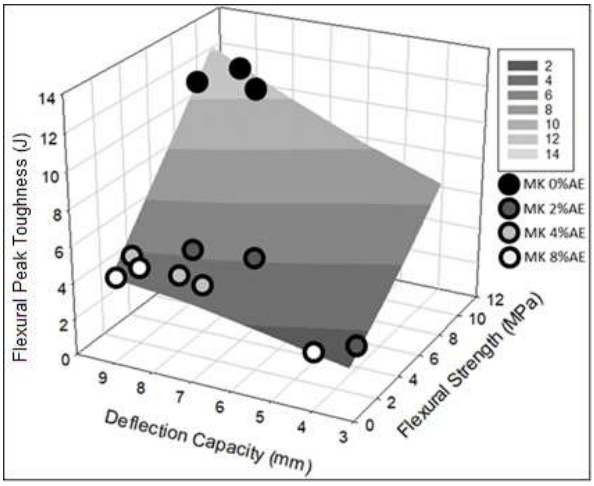

Fig. 12 - Flexural peak toughness – flexural strength - deflection capacity relations of composites.

composites were ranged between 3.49-4.93 MPa while deflection capacities were ranging between 3.80-9.91 mm. By taking the results into account, the flexural peak toughness values of air entrained composites were much affected by deflection capacity. MK 4%AE series presented best results within the air entrained composites due to more robust flexural behavior (low standard deviations).

The effect of AE dosage to the cracks number and average crack widths of composites

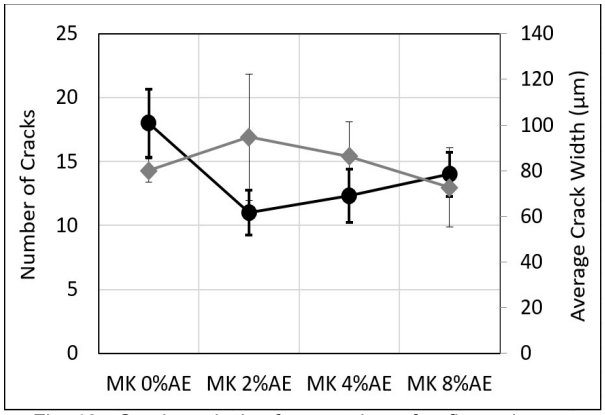

Fig. 13 - Crack analysis of composites after flexural tests.

were given in Figure 13. With the addition of AE, crack numbers were decreased when compared to control composite. However, the crack numbers of composites were gradually increased by increased AE dosages. Depending on the increased crack numbers, average crack widths of composites were also decreased (Figure 13).

3.3.2 Tension Test Results

The stress – strain graphs, first cracking/flexural strengths and strain capacities of composites were given in Figure 14a and Figure 14b, respectively. Observations for first crack/tensile strength can be made by using the left axis; strain observations can be made by using the right axis of Figure 14b.

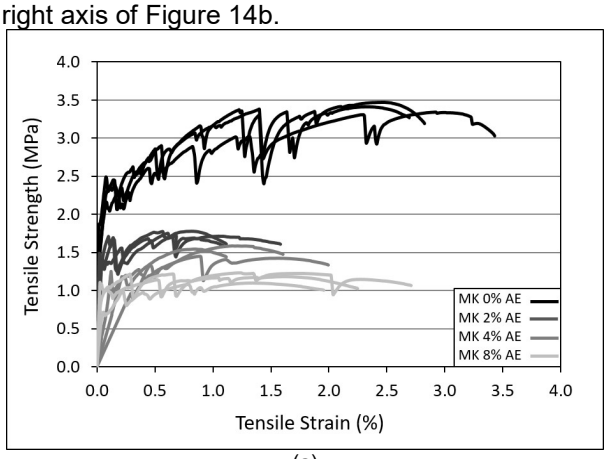

(a)

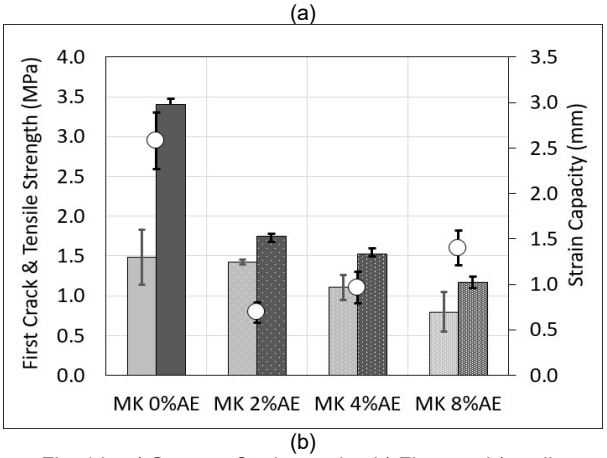

(b)

Fig. 14 - a) Stress – Strain graphs, b) First crack/tensile strengths and strain capacities of composites.

Similar results to flexural tests but more robust in terms of standard deviation were observed (Figure 14a and Figure 14b). First crack and tensile strengths of composites were significantly decreased at 2% AE dosage. Increasing the AE dosage over 2% gradually decreased both first crack and tensile strengths (Figure 14b). A remarkable decrease in terms strain capacity was also occurred by use of 2% AE. However, increasing the AE dosage over 2% gradually increased the strain capacity of composites (Figure 14b).

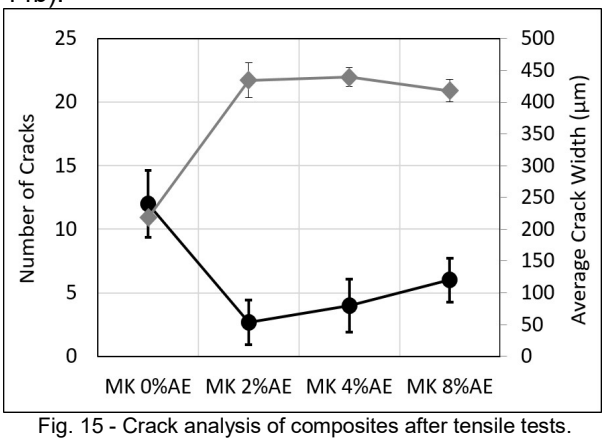

Fig. 15 - Crack analysis of composites after tensile tests.

The cracks number and average crack widths of composites were also measured after tensile tests (Figure 15). Similar results to the flexural tests were obtained. Crack numbers of composites were remarkably decreased while average crack widths were increased with the addition of air entraining admixture when compared to control composite. However, the crack numbers of composites were gradually increased by increased air entraining admixture dosages (Figure 15).

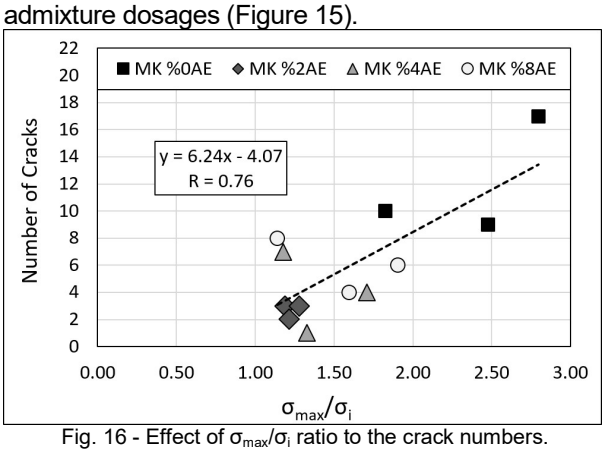

Fig. 16 - Effect of σ_{max}/σ_i ratio to the crack numbers.

According to theory of micro-mechanics purposed by Li [16], when the ratio of tensile strength to first crack strength (σ_{max}/σ_i) is increased, it is envisaged that the multiple cracking behavior will be enhanced. By taking this criterion into consideration, the effect of σ_{max}/σ_i ratio to the crack number was investigated (Figure 16). A positive correlation between σ_{max}/σ_i ratio and the number of cracks was calculated.

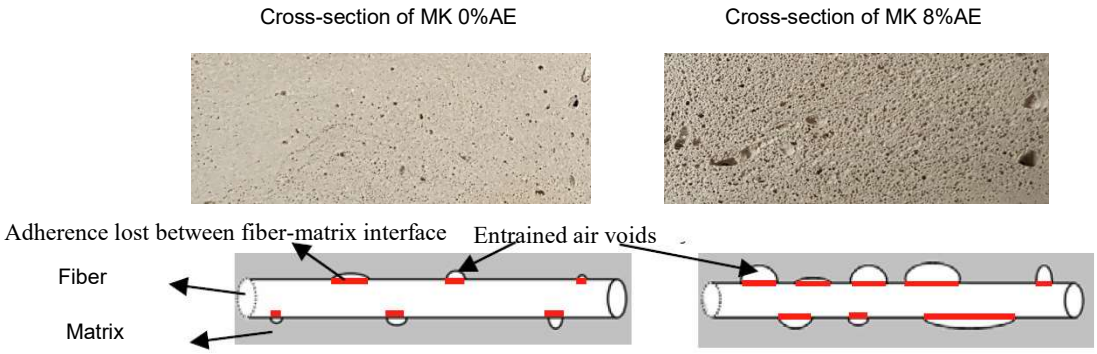

Fig. 17 - Loss of adherence between the fiber-matrix interface (schematically).

Average crack widths of composites were decreased slightly by increased crack numbers (Figure 15). However, it was also observed that the average crack widths of tensile composites were prominently higher than the average crack widths of flexural composites. This situation can be clarified by loading conditions, crack numbers and adherence between the fiber-matrix. In flexural tests, compression zone can prevent the crack propagation therefore the crack widths can be restricted. In tensile loading conditions, when crack occurred, tensile stresses in the cracked sections was corresponded directly by the polymeric fibers. If there is no significant number of cracks, these stresses cause the crack to widen by forming stress concentration. Besides, by adding AE, entrained air voids were formed on the interface between fiber and matrix which decreases the frictional bond between the matrix and fiber (schematically visualized in Figure 17). As a second result of decreased fiber-matrix adherence, stresses cannot be transferred to the non-cracked sections of composites effectively which also prevent new crack formations. Due to the reasons mentioned, crack widths were increased in tensile tests up to 400-450 μm.

3.3.3 Compressive Test Results

Compression test results of composites were presented in Figure 18. In control composite, a compressive strength of 45 MPa was obtained. Compressive strengths of composites were decreased by increased air entraining admixture dosage. 61, 79 and 85% of reduction in compressive strengths were calculated for 2, 4 and 8% of air entraining admixture dosages, respectively.

3.4 Thermal Test Results

Thermal conductivity results of composites measured from the thermal conductivity tests were given in Figure 19a. Conductivity of any material can be correlated with the dry density of the material, commonly. Dry density - Thermal conductivity relations of composites were also given in Figure 19b. In addition to the literature, thermal permeability results of composites

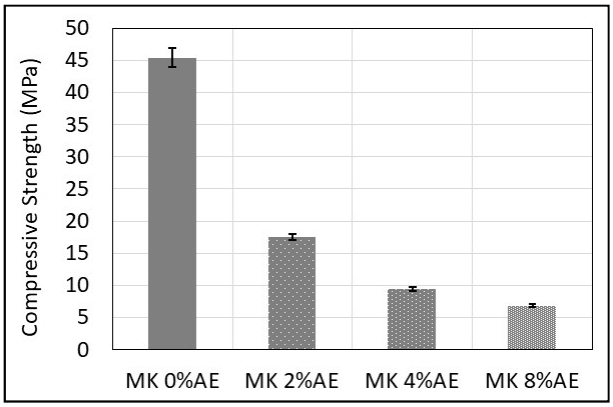

Fig. 18 - Compressive strengths of composites

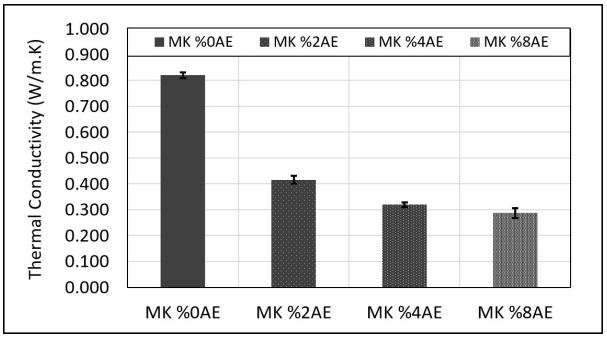

(a)

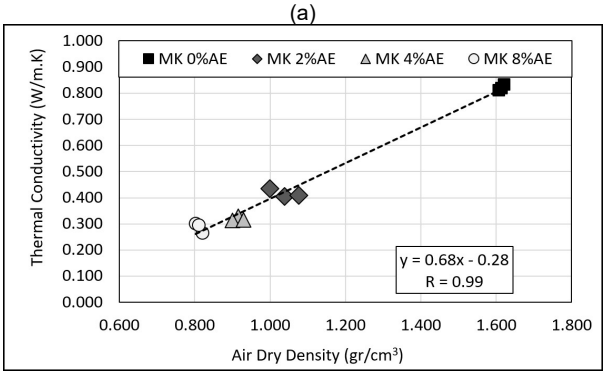

(b)

Fig. 19 - a) Thermal conductivities of composites, b) Thermal conductivity – Air dry density relation.

(ultimate surface temperatures, USTs (Figure 20)) were correlated with the thermal conductivity results of composites (Figure 21).

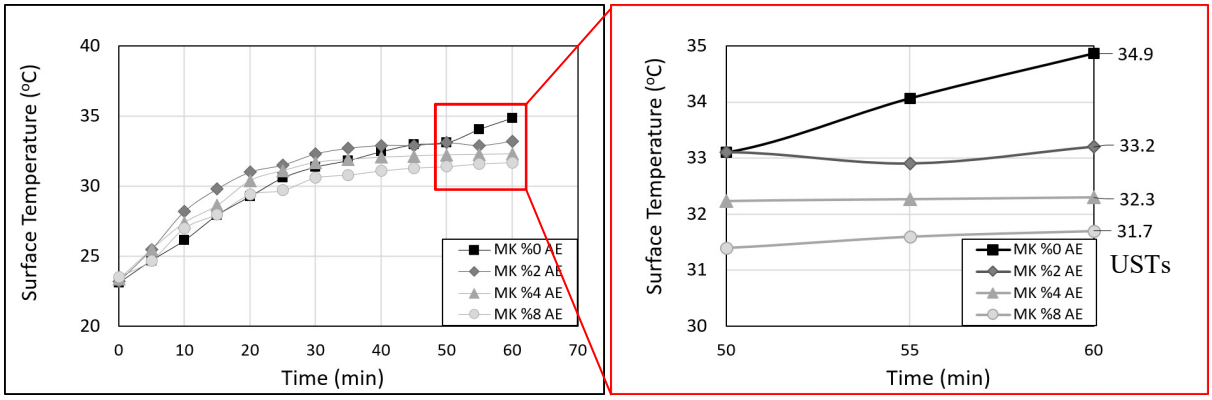

(a) (b)

Fig. 20 - a) Thermal permeability test results of composites, b) USTs of composites

Thermal conductivity of control composites were ranged between 0.811-0.833 W/m.K which was already lower when compared to the thermal conductivity coefficient of conventional concrete obtained from the literature [17]. Thermal conductivities of composites were further decreased by use of air entraining admixture down to 0.288 W/m.K, effectively (Figure 19a). By use of 2, 4 and 8% of AE, thermal conductivities were decreased by 49, 61 and 65%, respectively (Figure 19a). Commonly, positive correlation between the air dry density and thermal conductivity values were observed (R=0.99) (Figure 19b).

Average surface temperatures (AST) of composites were presented in Figure 20, by 5 min intervals. AST value of control composite gradually increased by time and at 60 min no saturation point was observed, AST curve continued to increase (Figure 20a). However, in terms of air entrained composites, after 50 min of heat exposure no significant changes were observed on surface temperature of composites (Figure 20a). After 50 min heat exposure, surface temperatures were remained which were accepted as ultimate surface temperatures (USTs) (Figure 20b). In terms of USTs, UST values of composites were decreased with air entraining admixture dosage. Since low UST represent low to thermal permeability, high resistance to thermal permeability was obtained with increasing air entraining dosage.

The correlation between the thermal conductivity and UST data for each composite were investigated (Figure 21). Positive correlation was found and a high correlation coefficient was calculated as R=0.96.

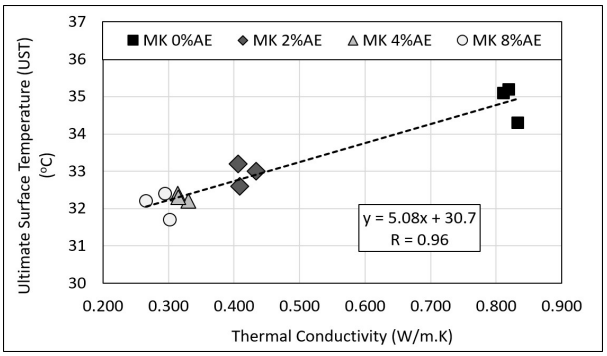

Fig. 21 - Thermal conductivity – Ultimate surface temperature correlation of composites.

4. Conclusions and possible application areas of HTP-LECC

In this study, the first lightweight ECC incorporating HTP fiber was successfully produced by use of air entraining admixture in ratios of 0, 2, 4 and 8% by cement weight. Following results were concluded;

-As expected, the amounts of entrained air in composites were increased by air entraining admixture dosage.

-Lightweightness of composites were measured by aerometer tests and the accuracy of the aerometer test was confirmed by image processing technique. Composites were lightweightened by 19-35% by use of AE.

-AE dosage positively affected the rheological properties of cement matrix. AE decreased both the τ_0 and η when compared to control matrix. Relatively lower values of τ_0 and η were observed for the case of 8% AE at both 0 and 45 min rheological tests. Use of higher AE dosage was found advantageous in terms of preventing the loss of consistency.

-When AE introduced to the composites, deformation capacities (deflection and strain capacity) of composites were decreased when compared to control composites (MK 0%AE). However, deformation capacities of HTP-LECCs were increased by increasing admixture dosage within air entrained composites under both flexural and tensile loading conditions.

-First crack (in both flexural and tensile loading conditions), flexural, tensile and compressive strengths of composites were significantly decreased by increasing AE.

-Flexural peak toughness values of composites were enhanced by increasing flexural strength and deflection capacity.

-Decreased crack numbers and increased crack widths were obtained by use of AE when compared to control composites. Crack numbers of composites were increased by increased AE dosage while crack widths were decreased in both flexural and tensile cases.

-In tensile tests, numbers of cracks were increased by increasing σ_{max}/σ_i ratio and a positive correlation between σ_{max}/σ_i ratio and the number of cracks was calculated.

-In flexural tests, compression zone prevents the crack propagation which also restricts crack widths. In tensile loading conditions, crack widths were increased up to 400-450 μm. Tensile stresses in the cracked sections was corresponded directly by the polymeric fibers. Owing to that, crack widths are directly affected by fiber distribution properties and the adherence between the fiber-matrix interface. In this study, it has been visually proved that entrained air voids were formed on the fiber-matrix interface by adding AE, which decreases the frictional bond between the matrix and fiber and increases crack widths as a drawback of the study in terms of durability.

-Thermal conductivities of composites were decreased by increasing AE dosage remarkably in positive manner. 50-65% better thermal conductivity performance was obtained when compared to control composite. Strong correlation between air dry density and thermal conductivity was found, commonly.

-A novel thermal camera test setup was used for the determination of thermal permeability of composites. Strong correlation was found between thermal conductivity and thermal permeability tests.

Following suggestions can be purposed for possible use area of HTP-LECCs by taking both mechanical and thermal properties into account:

-Even at the control composites, enhanced mechanical and thermal properties were obtained. Therefore, MK 0%AE composite can be used in structural application for ensuring both improved strength, deformation and thermal performances.

-MK 2%AE and MK 4%AE composites can be used in non-load bearing partition wall system owing to their considerable compressive strength and thermal conductivity.

-MK 8%AE is preferred for the use of non-load bearing building envelope systems owing to its lowest thermal conductivity and highest resistance to thermal permeability when compared to other composites.

ACKNOWLEDGEMENT

Materials supply from Çimentaş (cement), WR Grace Company U.S. (HRWRA and Air entraining admixture), and Saint-Gobain Brasil (HTP fiber) are gratefully acknowledged. The cooperation of Civil Engineer Tevfik Hakan BOZKURT is also acknowledged. Authors specially thanks to Associate Professor Mete Kun for his help in using the thermal permeability test equipment.

REFERENCES

1. V.C. Li and T. Kanda, Innovations forum: engineered cementitious composites for structural applications, Journal of Materials in Civil Engineering, 1998, **10**(2), 66-69.
2. M. Maruta, T. Kanda, S. Nagai and Y. Yamamoto, New high-rise RC structure using pre-cast ECC coupling beam, Concrete Journal, 2005, **43**(11), 18-26.
3. K. Rokugo, T. Kanda, H. Yokota and N. Sakata, Applications and recommendations of high performance fiber reinforced cement composites with multiple fine cracking (HPFRCC) in Japan, Materials and Structures, 2009, **42**(9), 1197.
4. S. Wang and V.C. Li, Materials design of lightweight PVA-ECC, Proceedings of HPFRCC, 2003, 379-390.
5. X. Huang, R. Ranade, Q. Zhang, W. Ni and V.C. Li, Mechanical and thermal properties of green lightweight engineered cementitious composites, Construction and Building Materials, 2013, **48**, 954-960.
6. Y. Wu, J.Y. Wang, P.J. Monteiro and M.H. Zhang, Development of ultra-lightweight cement composites with low thermal conductivity and high specific strength for energy efficient buildings, Construction and Building Materials, 2015, **87**, 100-112.
7. Z. Chen, J. Li and E. Yang, High strength lightweight strain-hardening cementitious composite incorporating cenosphere. In 9th International Conference on Fracture Mechanics of Concrete and Concrete Structures, 2016, pp. 1-8.
8. Q. Zhang and V.C. Li, Development of durable spray-applied fire-resistive Engineered Cementitious Composites (SFR-ECC). Cement and Concrete Composites, 2015, **60**, 10–16. doi:10.1016/j.cemconcomp.2015.03.012
9. xxx, ASTM C260/C260M-10a:2016 Standard Specification for Air-Entraining Admixtures for Concrete, ASTM International, West Conshohocken, PA, www.astm.org
10. M. Schatzmann, G.R. Bezzola, H.E. Minor and P. Fischer, The ball measuring system—a new method to determine debris-flow rheology. Debris-Flow Hazards Mitigation: Mechanics, Prediction and Assessment: Rotterdam, Millpress, 2003, 387-398.
11. M. Schatzmann, PhD Thesis, Rheometry for large particle fluids and debris flows, ETH Zurich, 2005.
12. xxx, ASTM C231/C231M-17a:2017 Standard Test Method for Air Content of Freshly Mixed Concrete by the Pressure Method, ASTM International, West Conshohocken, PA, 2017, www.astm.org, doi: 10.1520/C0231_C0231M-17A
13. xxx, ASTM C1113/C1113M-09:2009 Standard Test Method for Thermal Conductivity of Refractories by Hot Wire (Platinum Resistance Thermometer Technique), ASTM International, West Conshohocken, PA, www.astm.org.
14. K. Tosun-Felekoglu and B. Felekoglu, Effects of fibre hybridization on multiple cracking potential of cement-based composites under flexural loading, Construction and Building Materials, 2013, **41**, 15-20.
15. S.H. Park, D.J. Kim and S.W. Kim, Investigating the impact resistance of ultra-high-performance fiber-reinforced concrete using an improved strain energy impact test machine. Construction and Building Materials, 2016, **125**, 145-159.
16. V.C. Li, Engineered cementitious composites-tailored composites through micromechanical modeling, Fiber Reinforced Concrete: Present and the Future, Canadian Society of Civil Engineers, 1997, edited by N. Banthia, A. Bentur, and A. Mufti, p. 38
17. A.M. Neville, Properties of Concrete, Longman Scientific and Technical, 1995, p. 844.

****